Lab on a Chip

PAPER

View Article Online
View Journal | View Issue

Cite this: *Lab Chip*, 2024, **24**, 4581

Development of *in vitro* model of exosome transport in microfluidic gut-brain axis-on-a-chip

Gwang Myeong Seo,[a] Hongki Lee,[b] Yeon Jae Kang,[a] Donghyun Kim *[b] and Jong Hwan Sung *[a]

Received 4th June 2024,
Accepted 20th August 2024

DOI: 10.1039/d4lc00490f

rsc.li/loc

The gut communicates with the brain in a variety of ways known as the gut–brain axis (GBA), which is known to affect neurophysiological functions as well as neuronal disorders. Exosomes capable of passing through the blood–brain-barrier (BBB) have received attention as a mediator of gut–brain signaling and drug delivery vehicles. In conventional well plate-based experiments, it is difficult to observe the exosome movement in real time. Here, we developed a microfluidic-based GBA chip for co-culturing gut epithelial cells and neuronal cells and simultaneously observing exosome transport. The GBA-chip is aimed to mimic the *in vivo* situation of convective flow in blood vessels and convective and diffusive transport in the tissue interstitium. Here, fluorescence-labeled exosome was produced by transfection of HEK-293T cells with CD63-GFP plasmid. We observed in real time the secretion of CD63-GFP-exosomes by the transfected HEK-293T cells in the chip, and transport of the exosomes to neuronal cells and analyzed the dynamics of GFP-exosome movement. Our model is expected to enhance understanding of the roles of exosome in GBA.

1. Introduction

The connection between the gut and the brain, mediated by multiple pathways involving chemical signalling and the enteric nervous system, has been known since the 1800s and referred to as the Gut-Brain-Axis (GBA).[1–4] Recent research has unveiled various signalling pathways within the GBA,[5] and chemical signalling is one of the major pathways. For example, glucagon-like peptide 1 (GLP-1) secreted in the gut can traverse the blood–brain barrier (BBB) and bind to GLP-1 receptors in the brain, influencing appetite regulation.[6,7] Furthermore, gut microbiota plays a pivotal role in brain function and its involvement in neurological disorders. Notably, short-chain fatty acids (SCFA), like butyrate, produced by gut microbiota, can restore BBB function when damaged by traumatic brain injury.[8] Additionally, *Escherichia coli*, a constituent of gut microbiota, is known to secrete curli proteins, which have been linked to an increased misfolding of α-synuclein, a pathological factor in Parkinson's disease.[9,10] Moreover, dysbiosis in gut microbiota has been associated with the onset of depression.[11,12] Given the significance of these interactions, the GBA emerges as a critical area of exploration in the context of understanding brain disorders and functions, making it a subject of profound importance.

Exosomes, a subtype of extracellular vesicles (EV), are actively secreted by cells into the extracellular environment. They typically exhibit sizes ranging from 50 to 200 nm and are enriched with various components, including nucleic acids and proteins. These distinctive features underscore the pivotal role of exosomes as intercellular messengers within the body, capable of triggering diverse physiological responses such as cell differentiation and apoptosis.[13–15] Recent investigations in the field of gut–brain-axis (GBA) research have shed light on the multifaceted applications and functions of exosomes as signalling mediators.[16–20] Notably, exosomes possess the unique ability to traverse the blood–brain barrier, rendering them promising candidates for delivery vehicles of oral therapeutics aimed at addressing neurological disorders.[18,19] For instance, Katakura and colleagues have provided evidence that exosomes secreted by human-derived intestinal cells, specifically Caco-2 cells cultured in a medium supplemented with gamma-aminobutyric acid (GABA), have the capacity to induce the differentiation of brain neuroblastoma cells, such as SH-SY5Y cells.[21] These findings underscore the substantial potential of exosomes as versatile signalling agents with implications for GBA interactions and neurological therapeutics.

Recent investigations into the GBA and exosomes have predominantly relied on *in vivo* experimentation and *in vitro* studies conducted in conventional well plates.[21,22] For

[a] *Department of Chemical Engineering, Hongik University, Seoul, 04066, Republic of Korea. E-mail: jhsung22@hongik.ac.kr*
[b] *School of Electrical and Electronic Engineering, Yonsei University, Seoul, Korea 03722*

instance, Katakura and his team cultured Caco-2 and SH-SY5Y cells separately in individual well plates, isolating exosomes released by Caco-2 cells, and subsequently introducing them to SH-SY5Y cells.[21] Similarly, Liu and his colleagues have confirmed that exosomes secreted from the intestines under conditions of induced intestinal ischemia–reperfusion interact with microglia, resulting in brain injury. To explore this phenomenon, they collected exosomes from the intestines of mice subjected to induced intestinal ischemia/reperfusion and introduced them to HT-22 cells (mouse hippocampus neuronal cells) cultured in a well plate.[22] However, both *in vivo* and cell-based *in vitro* experiments have several limitations. Ethical concerns surround the use of animal models, and well plate experiments are labor-intensive, involving the purification of exosomes secreted by donor cells and their subsequent introduction to recipient cells. Importantly, these approaches fall short in studying the dynamics of exosome transport and real-time impact of exosomes on target cells after their release and transport.

To address these challenges, organ-on-a-chip platforms, capable of emulating human-like environments and facilitating real-time cell interactions *via* microfluidic channels, is gaining attention. Many organ-on-a-chip systems have been developed, aiming to reproduce the tissue-specific microenvironment and functions of various organs.[23] Based on recent progress in the organ-on-a-chip field, there have been attempts to develop microfluidic-based organ-on-a-chip systems aimed at reproducing the action of exosomes *in vivo*. In a study by Oh *et al.*, authors developed a microfluidic chip featuring a collagen channel, which enabled the co-culture of both differentiated F11 (mouse neuroblastoma cells) and undifferentiated F11 cells, thus fostering interactions mediated by exosomes.[24] This microfluidic chip was designed to incorporate channel reservoirs of varying sizes for differentiated F11 cells and undifferentiated F11 cells, resulting in a gradient effect due to differential evaporation. Consequently, this resulted in a microfluidic chip featuring convection, facilitating the observation of exosome transportation driven by convection flow. Nevertheless, it has its drawbacks, as it is based on a single cell type (mouse neuroblastoma cells) and does not utilize human cells.

In a previous investigation into the interactions between the gut epithelium and the brain endothelium *via* exosomes, our group designed a bilayered organ-on-a-chip that enabled the co-culture of intestinal cells in the upper layer and brain vascular endothelial cells in the lower layer.[25] Initially, intestinal cells were cultured in a conventional well plate. Subsequently, exosomes were extracted, fluorescently labelled, and introduced into the layer where intestinal cells of the organ-on-a-chip were being cultivated. As a result, we observed the transport of exosomes across the intestinal barrier, ultimately reaching the brain vascular cells. This method allowed for the quantitative confirmation of exosome passage through the intestinal barrier. However, it is important to note that the process of isolating and purifying exosomes proved to be labor-intensive, and real-time monitoring of exosome dynamics was restricted.

Here, we aimed to address previous research limitations by developing a GBA chip that enables co-culture of intestinal and brain nerve cells and real-time observation of exosome secretion from intestinal cells and their transfer to brain nerve cells (Fig. 1A and B). Previous studies have shown that convective flow is more important than diffusion for delivering exosomes released from cells to other cells.[24] In this study, we designed and compared two types of GBA chips. The first one is the GBA-convection chip, which emulates convective flow like interstitial flow in the body. The second one is the GBA-diffusion chip, where transport is predominantly governed by diffusion. We carried out a comparative evaluation of substance transport using these two chips (Fig. 1C). Caco-2 cells, human intestinal cells, were cultured in the gut channel of the GBA-convection chip, and SH-SY5Y cells, human neuroblastoma cells, were cultured in the brain channel. We confirmed the co-culture of intestinal and brain nerve cells. To validate the transport of exosomes in the GBA chip, HEK-293T cells transfected with the CD63-GFP plasmid were cultured in the gut channel. We observed the fluorescent exosomes released from these cells moving into the brain channel and interacting with SH-SY5Y cells.

2. Materials and methods

2.1 Fabrication of GBA chip

The GBA chip is a microfluidic device consisting of two channels for cell culture and one channel for filled with collagen hydrogel, all parallel to one another. Two channels capable of culturing gut and brain cells were named as the "gut channel" and "brain channel", respectively. The central channel was labelled as the "collagen gel channel" (Fig. 1A). The width of the collagen gel channel is 1300 μm, while the gut channel and brain channel are present on both sides of the collagen gel channel, each with a width of 400 μm (Fig. 1B).

To fabricate the GBA chip, we utilized the soft lithography method. Initially, we coated a silicon wafer with SU-8 and used photolithography techniques to imprint the GBA chip pattern, creating a master mold. We mixed polydimethylsiloxane (PDMS) prepolymer (Sylgard 184; Dow Corning Corp, USA) at a 10 : 1 weight-to-weight ratio to create a PDMS mixture, which was then poured into the master mold. The master mold was placed in a vacuum chamber for degassing, and then left overnight at 60 °C for curing. After removing the cured PDMS from the master mold, reservoirs for each channel were made using biopsy punches. The gut channel in the GBA-convection chip (Fig. 1C(i)) had a diameter of 3 mm, while the collagen gel channel and brain channel reservoirs were created using biopsy punches with a diameter of 1 mm. In the GBA-diffusion chip (Fig. 1C(ii)), both the gut channel and brain channel reservoirs had a diameter of 3 mm, and the collagen gel channel was established with a diameter of 1 mm, also using biopsy

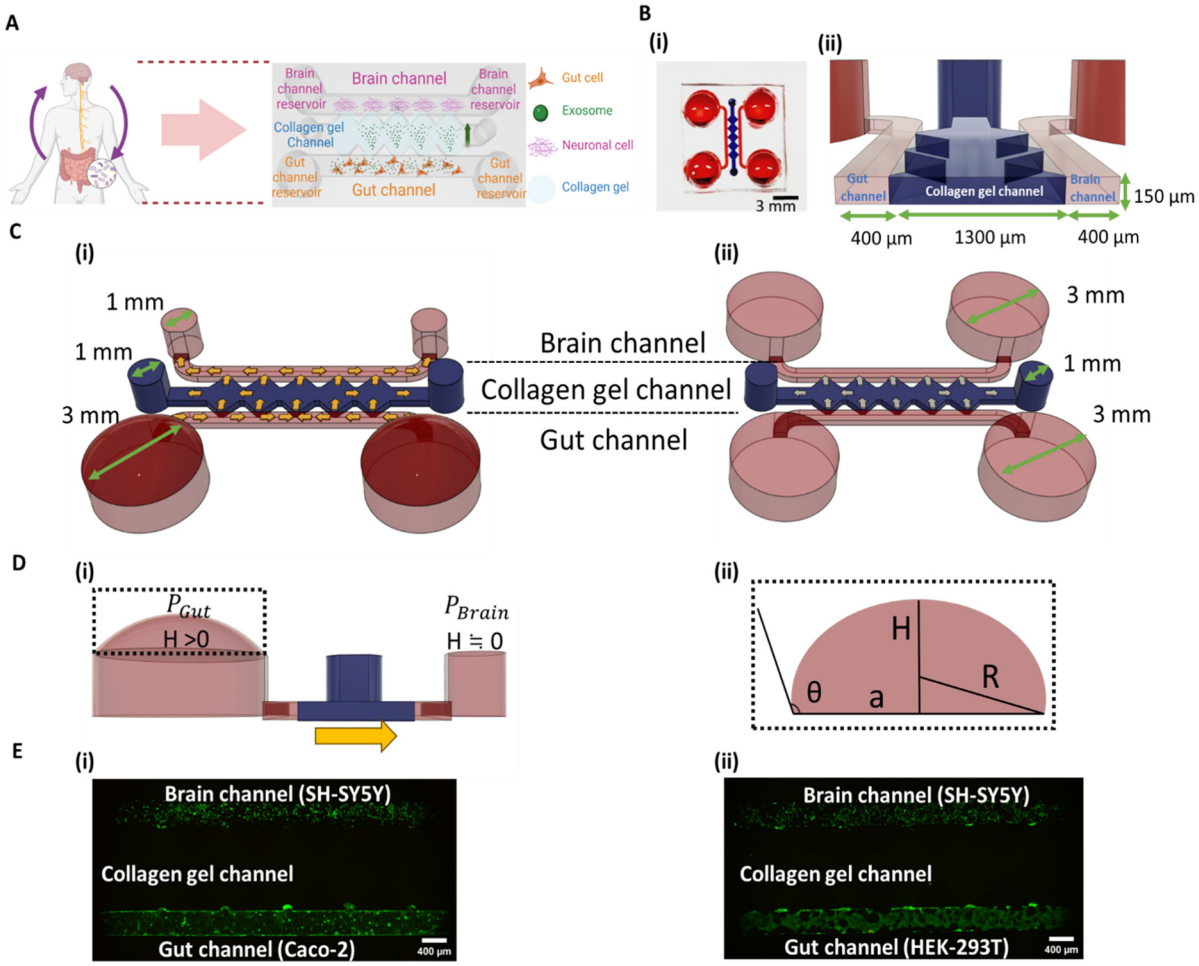

Fig. 1 The design of *in vitro* GBA-chip and cell co-culture. Scheme of *in vitro* GBA chip. (A) Scheme of *in vitro* GBA chip. (B) Design of GBA chip and picture. (i) GBA chip picture. (ii) GBA chip design. (C) Fluid flow and diffusion direction in GBA chip. (i) GBA-convection chip. (ii) GBA-diffusion chip. Yellow arrow: convection and diffusion flow in GBA-convection chip. Gray arrow: diffusion flow in GBA-diffusion chip. (D) Scheme of convection flow using surface tension in GBA-convection chip. P_{Gut} is pressure of gut channel reservoir. P_{Brain} is pressure of brain channel reservoir. (i) Image of convection flow generated by droplet. (ii) The geometric image of droplet in gut channel reservoir. *R* is the radius of the droplet. *H* is the droplet height. *a* is the half chord length. Θ is the contact angle. (E). Co-culture for 24 h and Live/Dead assay in GBA-convection chip. (i) Caco-2 and SH-SY5Y co-culture. (ii) HEK-293T and SH-SY5Y co-culture. Green: live cell, Red: dead cell.

punches (Fig. 1C). The PDMS layer with the GBA chip pattern and the slide glass were subjected to oxygen plasma treatment (CUTE; Femto Science, Korea) at 70 W for 60 seconds. After the treatment, the PDMS layer and slide glass were bonded together by manually aligning the two layers.

2.2 Cell co-culture in GBA-convection chip

The intestinal cells used were human colorectal adenocarcinoma cells (Caco-2; ATCC, HTB-37, USA), for the fluorescent exosome secretion experiment, human embryonic kidney cells (HEK-293T; ATCC, CRL-3216, USA) were used, and for the brain nerve cells, human neuroblastoma cells (SH-SY5Y; Korean cell line bank, 22266, Korea) were utilized. All cells were cultured in Dulbecco's modified Eagle medium (DMEM; Gibco, 11995-040, USA) supplemented with 10% fetal bovine serum (FBS; Welgene, S001-01, Korea) and 1% penicillin–streptomycin (P/S; Sigma-Aldrich, P4333, USA) at 37 °C in a 5% CO_2 incubator. The culture media were changed every 2–3 days.

To make a 2.0 mg ml^{-1} collagen solution for injection into the collagen gel channel of the GBA-convection chip, rat tail type 1 collagen (Corning, 354236, USA) of 3 mg ml^{-1} concentration was prepared using 1 N NaOH (SAMCHUN CHEMICALS, S1996, Korea) and 10× Dulbecco's phosphate buffered saline (10× DPBS; Sigma-Aldrich, D5652, USA). The 3 mg ml^{-1} collagen solution was then diluted with distilled water to the final concentration of 2 mg ml^{-1}. After injecting 2.0 mg ml^{-1} collagen into the collagen gel channel of the GBA-chip, it was incubated for 30 minutes in a 37 °C, 5% CO_2 incubator. Following gelation of the collagen, a 1 mg ml^{-1} concentration of fibronectin (Sigma-Aldrich, F1141, USA) was introduced into both the gut channel and the brain channel. Subsequently, it was incubated for 1 hour at 37 °C with 5% CO_2. The gut channel and brain channel were washed once with PBS, and then both channels were filled

with medium. In the Brain channel, SH-SY5Y cells were injected at a concentration of 7×10^6 cells per mL, with a total volume of 20 μL, and incubated at 37 °C with 5% CO_2 for 24 hours. Following this incubation, 60 μL of Caco-2 cells at a concentration of 1×10^7 cells per mL or 60 μL of HEK-293T cells at a concentration of 7×10^6 cells per mL was introduced into the gut channel of the device. In the gut channel, either Caco-2 or HEK-293T cells were seeded, while in the brain channel, SH-SY5Y cells were cultured. The co-culture was incubated at 37 °C with 5% CO_2 for 24 hours.

2.3 Transfection and exosome isolation

HEK-293T cells were seeded in a 6-well plate at a concentration of 2.5×10^5 cells per well and cultured for 24 hours at 37 °C with 5% CO_2. After 24 hours, a diluted DNA total solution was prepared by adding 2.5 μg of pCT-CD63-GFP plasmid (System Biosciences, CYTO120-PA-1, USA) and 5 μL of Lipofectamine 3000 (Invitrogen, L3000001, USA) to 125 μL of Opti-MEM (Gibco, 31985-062, USA). The diluted Lipofectamine 3000 solution, prepared by adding 5 μL of Lipofectamine 3000 to 125 μL of Opti-MEM, was mixed with the diluted DNA total solution in a 1 : 1 ratio and incubated at room temperature for 5 minutes. The mixture of diluted Lipofectamine 3000 and diluted DNA total solutions in a 1 : 1 ratio (250 μL) was added to the 6-well plate containing HEK-293T cells, followed by overnight incubation at 37 °C with 5% CO_2. After overnight incubation, the transfected HEK-293T cells can be observed under a fluorescence microscope (Nikon, Eclipse Ti2-U inverted microscope, Japan), confirming the expression of fluorescence. To extract the CD63-GFP exosomes secreted by transfected HEK-293T cells, the culture medium of transfected HEK-293T cells was first replaced with DMEM containing 10% exosome-depleted fetal bovine serum qualified One Shot (exo-dep FBS; Gibco, A2720803, USA), and 1% P/S, followed by 2 days of incubation at 37 °C with 5% CO_2. After a 2 day incubation period, the culture medium containing transfected HEK-293T cells was harvested and subjected to centrifugation at 2000 × *g* for 30 minutes to eliminate cellular debris. The clarified medium, devoid of cell debris, was combined with Total Exosome Isolation Reagent (Invitrogen, 4478359, USA) at a volumetric ratio of 2 : 1. The mixture was then added to the cells, and the co-culture was incubated overnight at 2–8 °C. Following the overnight incubation, the culture was subjected to centrifugation at 10 000 × *g* for 1 hour. The supernatant was carefully aspirated, and the resulting exosome pellet was resuspended in PBS. To assess the size and distribution of the extracted CD63-GFP exosomes, dynamic light scattering (DLS) equipment (Malvern Panalytical, Nano S90 ZEN1690, UK) and Zetasizer software (Malvern Panalytical, UK) were employed.

2.4 Transport of FITC-dextran and CD63-GFP in GBA chip

To compare the fluid flow and substance transport from the GBA-convection chip to the brain channel with the GBA-diffusion chip, The 4 kDa fluorescein isothiocyanate-dextran (FITC-dextran; Sigma-Aldrich, 46944, USA) was used as the molecular tracer. Collagen channels of both chips were infused with collagen gel at a concentration of 2.0 mg ml^{-1}, followed by a 30 minute incubation at 37 °C with 5% CO_2. In the brain channel reservoir of the GBA-diffusion chip, we introduced 26 μL of phosphate-buffered saline (PBS; Sigma, P3813) and simultaneously added 26 μL of FITC-dextran at a concentration of 0.5 mg ml^{-1} to the gut channel reservoir. Similarly, in the brain channel reservoir of the GBA convection chip, 8 μL of PBS was introduced, followed by the addition of 28 μL of FITC-dextran at a concentration of 0.5 mg ml^{-1} to the gut channel reservoir. This sequential process resulted in the formation of a 2 μL droplet within the gut channel's reservoir, composed of FITC-dextran at a concentration of 0.5 mg ml^{-1}. Fluorescence microscopy was employed to capture images of FITC-dextran within the collagen gel channel over time, and the analysis was performed using ImageJ (National Institutes of Health, USA).

To observe GFP-exosomes released from cells, transfected HEK-293T cells were introduced into the gut channel of both the GBA-diffusion chip and GBA-convection chip at a concentration of 7×10^6 cells per ml, with a volume of 30 μL. The cells were then cultured at 37 °C with 5% CO_2 for one day. In the GBA-convection chip, convection was initiated by introducing 28 μL of medium into the gut channel reservoir, forming a 2 μL droplet, while the brain channel reservoir received 8 μL of medium. In the GBA-diffusion chip, to simulate a prevailing diffusion scenario, an equal volume of 26 μL of medium was introduced into both the gut and brain channel reservoirs. Using the time-lapse functionality of a fluorescence microscope, we captured images of CD63-GFP exosome movement within the collagen gel channels of the GBA-diffusion chip and GBA-convection chip at 10 second intervals for 30 minutes. Subsequently, we analyzed the trajectory of exosome movement using ImageJ software.

2.5 Construction of COMSOL Multiphysics model

We developed COMSOL models for the movement of FITC-dextran and exosomes in a GBA chip using the Particle Tracing Module, Laminar Flow Module, and Transport of Diluted Species Interface in COMSOL Multiphysics (COMSOL Inc., USA). In the GBA convection chip COMSOL model, a Darcy's permeability value of 1×10^{-13} m^2 was utilized for the collagen gel channel. This value is known to result in a flow velocity of 3.0 μm s^{-1} within the collagen scaffold when subjected to a pressure difference (ΔP) of 40 Pa, as reported in ref. 26. The porosity of the collagen gel channel was set to 0.8, utilizing the previously reported value from ref. 27. The pressure in the gut channel reservoir, denoted as P_{Gut}, was assumed to be 45 Pa, while the pressure in the brain channel reservoir, denoted as P_{Brain}, was assumed to be 0 Pa, resulting in the application of a pressure difference (ΔP) of 45 Pa. By applying eqn (4) from prior research,[28] it was assumed that a droplet with a volume of 2.34 μL formed in a PDMS reservoir

with a diameter of 3.3 mm results in a pressure (P) of 45 Pa. Consequently, it was further assumed that a droplet with a volume of 2 μL in a 3 mm diameter gut channel reservoir would also lead to a pressure (P_{Gut}) of 45 Pa. It was assumed that the pressure (P_{Brian}) in the brain channel reservoir, where droplets do not form, would be 0 Pa. The diffusion coefficient ($D_{collagen}$) of 4 kDa FITC-dextran in the collagen gel channel was determined using Ogston's stochastic model.

$$D_{collagen} = D \times \exp\left(-\Phi^{\frac{1}{2}} \times \frac{r}{r_f}\right) \quad (1)$$

where D [m^2 s^{-1}] represents the diffusion coefficient, Φ is the volume fraction, r_f [m] is the radius of 4 kDa FITC-dextran, and r_f [m] is the radius of 2.0 mg ml^{-1} collagen fibers. The values used for each of these parameters are 1.35×10^{-10} m^2 s^{-1}, 0.125, 2.15 nm, and 200 nm, respectively, as reported in previous research.[29,30] The particle diameter and density applied to the exosome transport model were set to 200 nm and 1.13 mg ml^{-1}, respectively, based on the known values for exosome diameter and density.[13,31]

2.6 Fluorescence staining of cell and cell membrane

A live/dead assay was performed to assess the cell viability cultured in the gut channel and brain channel of the GBA convection chip. The Live/Dead solution, consisting of ethidium homodimer-1 (Invitrogen, E1169, USA) and calcein AM (Invitrogen, C34852, USA) in PBS at a final concentration of 4 μM, was injected with 60 μL into the gut channel and 20 μL into the Brain channel, followed by incubation at 37 °C with 5% CO_2 for 30 minutes. To confirm the interaction between CD63-GFP exosomes released by transfected HEK-293T cells and SH-SY5Y cells, the membrane of SH-SY5Y cells was stained. After removing the culture medium from the brain channel, two washes were performed using Hank's balanced salt solution (HBSS; Sigma, USA). Then, 20 μL of wheat germ agglutinin, Alexa Fluor 633 conjugate (WGA 633, Invitrogen, USA) at a concentration of 45 μg ml^{-1} was added, followed by a 10 minute incubation at 37 °C with 5% CO_2. After removing WGA-633, perform two washes with HBSS, and then replenish with the culture medium.

3. Results and discussions

3.1 Chip design and co-culture on chip

We have engineered a microfluidic-based GBA chip designed to co-culture the intestinal and brain neural cells and to enable their interaction *via* exosomes (Fig. 1A). The GBA chip comprises three parallel channels, with the central channel, designated as the collagen gel channel, serving as a physical barrier for the co-culture of intestinal and brain neural cells on either side of the channel walls (Fig. 1B). The collagen gel channel plays a critical role in maintaining the separation of cells in the gut channel and brain channel, preventing their mixing. This design allows the exosomes secreted by the cells in the gut channel to traverse the barrier, facilitating their movement towards the brain channel *via* both diffusion and convection. Exosomes, with a size of 200 nm, demonstrate a diffusion coefficient of approximately 1.073×10^{-12} m^2 s^{-1} in 2 mg ml^{-1} collagen,[24] signifying that it would take approximately 130 hours to travel 1 mm through diffusion alone. Therefore, the presence of convection flow is crucial for efficient exosome transport.[24] In this study, we developed two types of GBA chips for experimentation. One is the GBA-convection chip, where convection flow exists from the gut channel to the brain channel, and the other is the GBA-diffusion chip, where diffusion is the primary mechanism for transport (Fig. 1C).

We attempted to approximate the time it takes for exosomes secreted by intestinal cells to be delivered to neurons in the brain within the human body. According to previous studies, purified exosomes extracted from cells were administered into the mouse vein, and after 5 minutes, their presence in the brain was confirmed.[32] While the brain interstitial flow velocity in mice and humans are similar at approximately 12 μm min^{-1} and 10–20 μm min^{-1}, respectively, the circulation time of blood is known to be slower in humans, taking around 60 seconds compared to approximately 20 seconds in mice.[24,33,34] Considering the difference in the circulation time, we estimated that exosomes secreted by intestinal cells would take about 6–8 minutes to reach neurons in the brain in the human body. If we disregard the weight of exosomes, to achieve the previously assumed transit time (approximately 6–8 minutes) of exosomes within the human body using the GBA-convection chip, it is anticipated that the flow velocity in the 1.3 mm length collagen gel channel connecting the gut and brain channels should be approximately 2.7 μm s^{-1} to 3.6 μm s^{-1}. The collagen gel channel situated between the gut channel and the brain channel is a porous medium. Therefore, fluid flow through the porous medium due to convection can be analyzed using Darcy's law.[35]

$$\frac{Q}{A} = \frac{K\Delta P}{\mu L} \quad (2)$$

where Q [m^3 s^{-1}] represents the volumetric flow rate, A [m^2] stands for the average surface area of the gel scaffold, μ [Pa s] represents viscosity, K [m^2] is Darcy permeability, ΔP [Pa] indicates pressure difference, and L [m] is the length of the gel scaffold. When expressing Darcy's law in terms of velocity (v [m s^{-1}]), it can be represented as eqn (2) in the following manner.

$$v = \frac{K\Delta P}{\mu L} \quad (3)$$

Polacheck *et al.* observed that the application of a pressure difference (ΔP) of 40 Pa to a 2 mg ml^{-1} collagen scaffold, as defined by eqn (3), induces a flow within the collagen gel channel at a velocity of 3 μm s^{-1}. To determine ΔP in the GBA-convection chip, we employed the Young and Laplace law, which relates droplet size to pressure (P).

$$\Delta P = P_{Gut} - P_{Brain} = \frac{2\gamma}{R_{Gut\ droplet}} - \frac{2\gamma}{R_{Brain\ droplet}} \quad (4)$$

$$R = \frac{H^2 + a^2}{2H} \tag{5}$$

$$H = (1 - \cos\theta)R \tag{6}$$

$$a = R\sin\theta \tag{7}$$

$$v = \frac{K}{\mu L}\Delta P = \frac{2\gamma K}{\mu L}\left(\frac{1}{R_{\text{Gut droplet}}} - \frac{1}{R_{\text{Brain droplet}}}\right) \tag{8}$$

where, γ [N m^{-1}] is the droplet surface tension, R [m] is the droplet radius, H [m] is the droplet height, a [m] is the half chord length, and θ [°] is the contact angle. In the presence of a droplet in the reservoir, pressure (P) is induced due to the interplay of γ and R. In cases where there is no droplet or it flattens out, θ becomes 0, and R tends toward infinity, resulting in the pressure drop across the droplet's curved interface approaching zero. Additionally, by organizing eqn (3) and (4), governing the radius of droplets formed in the gut channel reservoir and brain channel reservoir, we derived eqn (8). Assuming the absence of droplet formation in the brain channel reservoir (ignoring $R_{\text{Brain droplet}}$), one can adjust the $R_{\text{Gut droplet}}$ to determine the value of v in the collagen gel channel (Fig. 1D). For example, to achieve v values of 4, 3, 2, and 1 μm s^{-1}, the corresponding $R_{\text{Gut droplet}}$ values should be set at 2.8, 3.74, 5.6, and 11.2 mm, respectively. Chen *et al.* experimentally verified that when a droplet with a volume of 2.34 μL forms in a PDMS reservoir with a diameter of 3.3 mm, the value of R is determined to be 3.01 mm, and P is approximately 45 Pa. Applying this to eqn (8), we calculated that when $R_{\text{Brain droplet}}$ is set to 0 mm (P_{Brain} = 0 Pa), and $R_{\text{Gut droplet}}$ is adjusted to 3.01 mm (P_{Gut} = 45 Pa), the velocity (v) is approximately 3.4 μm s^{-1}.[28] In summary, to initiate convective flow from the gut channel to the brain channel in the GBA-convection chip, we generated a 2 μL volume droplet in the gut channel reservoir.

To establish an *in vitro* GBA model, we co-cultured the human intestinal cell line, Caco-2 and the human neuroblastoma cell line, SH-SY5Y in the GBA-convection chip for 24 hours and assessed cell viability. The Caco-2 cells in the gut channel and the SH-SY5Y cells in the brain channel were physically separated by the collagen gel channel, ensuring that the two cell types remained isolated and were cultured only within their respective channels. The live/dead assay confirmed the viability of both Caco-2 and SH-SY5Y cells after 24 hours of co-culturing (Fig. 1E-i). In the fluorescently labelled exosome transfer experiment, both the HEK-293T cells, used as a cell model simulating the gut in place of Caco-2 cells, and the SH-SY5Y cells were co-cultured in the GBA-convection chip for 24 hours without any adverse effects on each other (Fig. 1E-ii). Our co-culture result resembles those conducted in the conventional well plate environment, as reported previously.[36,37]

3.2 Transport of FITC-dextran in GBA chip

We compared the transport of FITC-dextran in the GBA-convection chip and the GBA-diffusion chip (Fig. 2A and B). Time-dependent changes in FITC-dextran concentration within the Collagen gel channel of both the GBA-convection and GBA-diffusion chips were recorded using fluorescence microscopy. After 10 minutes in the GBA-convection chip, the normalized intensity value at position A–A′ exceeded 0.6. In the GBA-diffusion chip, after 40 minutes, the intensity at the same position was lower than 0.2 (Fig. 2C and D). In Fig. 2A-d, FITC-dextran movement in the brain channel was observed in both the $-x$ and $+x$ directions relative to the A–A′ line. This movement is attributed to the pressure difference between the gut channel and the brain channel reservoirs, resulting in the formation of convective flow, which is divided and flows into the reservoirs at both ends of the brain channel. Consequently, it is presumed that the presence of convective flow from the gut channel to the brain channel in the GBA-convection chip facilitated a swifter movement of FITC-dextran compared to the GBA-diffusion chip.

We developed and simulated COMSOL models to replicate substance transport within the GBA-convection and GBA-diffusion chips (Fig. 2E and F). The COMSOL model for the GBA-convection chip indicated that FITC-dextran reached the brain channel within 10 minutes, whereas in the GBA-diffusion chip, FITC-dextran did not reach the brain channel even after 40 minutes (Fig. 2G and H). The velocity along the A–A′ line predicted by the GBA-convection COMSOL model was estimated to be 3.4 μm s^{-1}, falling within the typical range of velocities found in human internal tissues, as mentioned earlier. In Fig. 2E and F, it is evident that in the GBA-convection COMSOL model, FITC-dextran undergoes simultaneous movement in both the $-x$ and $+x$ directions along the A–A′ axis, consistent with the GBA-convection chip experiment. The graphs in Fig. 2C and G depict the calculation of the area under the curve for the normalized intensity profiles of the GBA-convection chip and GBA-convection COMSOL model over a 10 minute period, resulting in values of 1.110 and 1.068, respectively. This observation indicates a comparable extent of movement for FITC-dextran over the course of 10 minutes in both the model and the experiment, confirming that the COMSOL model faithfully simulates the experimental condition. When comparing the experimental results with the COMSOL model, we conclude that the flow velocity generated by the droplet in the GBA-convection chip was within the desired range. Moreover, according to the eqn (8), it would be feasible to modulate the flow velocity within the collagen gel channel by adjusting the droplet's radius.

3.3 Expression of CD63-GFP exosome

To visualize the convection-driven movement of exosomes from the gut channel to the brain channel in the GBA-convection chip, we made cells capable of releasing

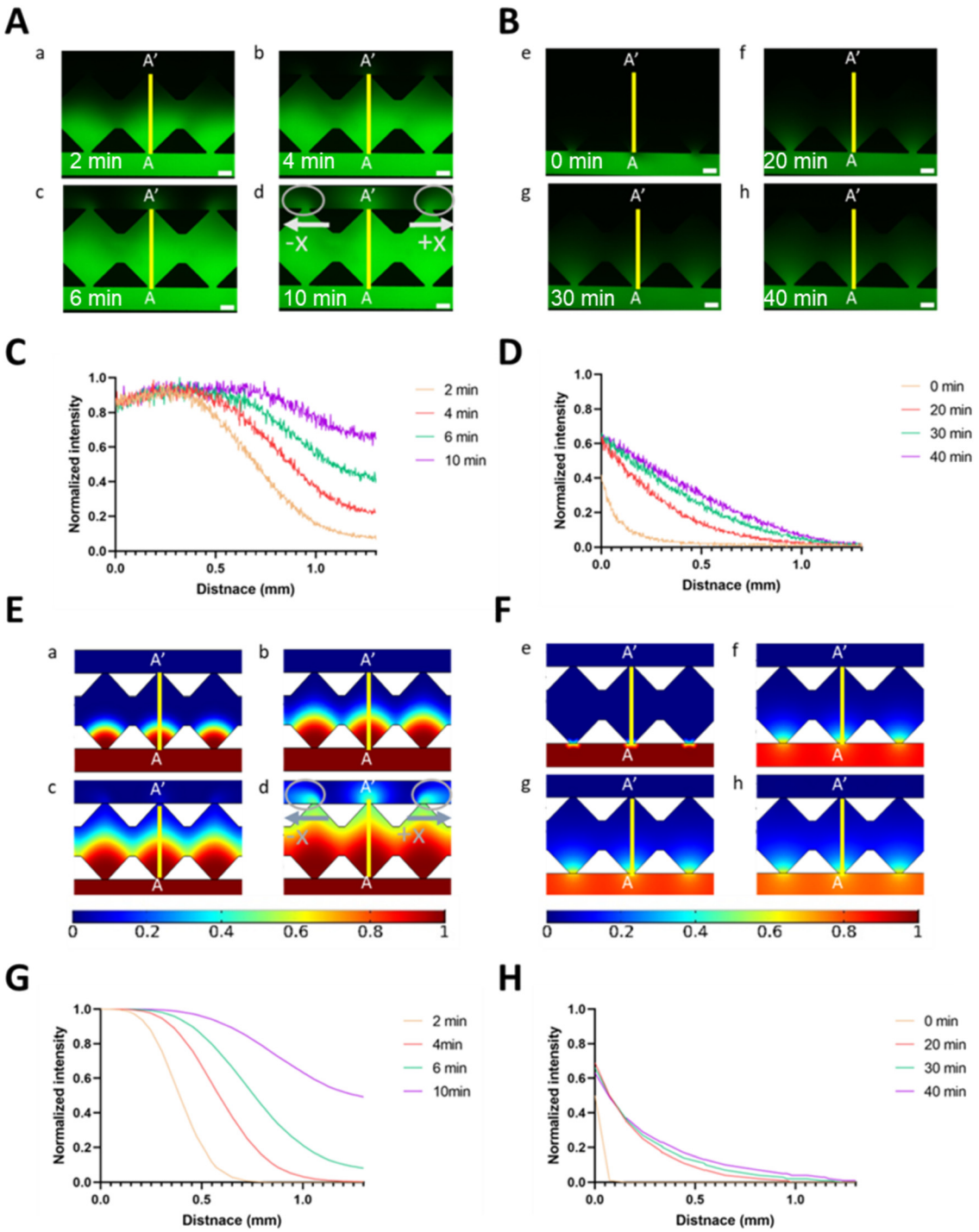

Fig. 2 Comparison of FITC-dextran transport in GBA-convection chip and GBA-diffusion chip. (A) Fluorescence images in GBA-convection chip by time. GBA-convection chip. (B) Fluorescence images in GBA-diffusion chip by time. GBA-diffusion chip. (C) Normalized intensity profile of FITC-dextran at the A–A′ line position over time in GBA-convection chip. (D) Normalized intensity profile of FITC-dextran at the A–A′ line position over time in GBA-diffusion chip. (E) Simulation results of FITC-dextran transport in GBA-convection chip COMSOL model by time. GBA-convection chip COMSOL model. (F) Simulation results of FITC-dextran transport in GBA-diffusion chip COMSOL model by time. GBA-diffusion chip COMSOL model. (G) Normalized intensity profile of FITC-dextran at the A–A′ line position over time in GBA-convection chip COMSOL model. (H) Normalized intensity profile of FITC-dextran at the A–A′ line position over time in GBA-convection chip COMSOL model. Time points a, b, c, and d correspond to 2, 4, 6, and 10 minutes, respectively, while e, f, g, and h correspond to 0, 20, 30, and 40 minutes, respectively. Scale bar 250 micrometers.

fluorescently labelled exosomes by transfecting HEK-293T cells with a plasmid that introduced fluorescent labelling of the CD63 protein on the exosome's surface. CD63 is a well-known tetraspanin protein located on exosome surfaces and is frequently used as an exosome marker.[38] Cells transfected with the CD63-GFP plasmid can secrete exosomes that are

fluorescently labelled, known as CD63-GFP exosomes.[39,40] Unfortunately, transfected Caco-2 cells did not effectively secrete fluorescently labelled exosomes, due to the limited transfection efficiency. Consequently, we opted to use HEK-293T cells, known for their transfection efficiency and the capacity to secrete CD63-GFP exosomes as a substitute for Caco-2 cells. HEK-293T cells are commonly employed in research related to exosome-based therapy for neurodegenerative diseases.[41,42] Ryosuke Kojima *et al.* encapsulated transfected HEK-293T cells capable of secreting exosomes containing catalase mRNA and implanted them into the subcutaneous tissue of living mice. This experiment demonstrated the alleviation of neuronal cell death and neuroinflammation.[41] Yavar Jahangard *et al.* transfected HEK-293T cells to secrete exosomes containing miR-29. When these exosomes were injected into the hippocampus of rats induced with Alzheimer's disease using amyloid beta, they observed the restoration of the rats' cognitive abilities.[42] Brian J. Jurgielewicz *et al.* confirmed the uptake of fluorescently labelled exosomes secreted by transfected HEK-293T cells by SH-SY5Y cells.[43]

Currently, there is a lack of specific explanations for differences in exosome secretion based on their originating organs. The known process of exosome secretion involves several key steps. Firstly, the endosome within the cell undergoes transformation into a multivesicular body (MVB) containing intraluminal vesicles (ILVs), a process facilitated by the action of endosomal sorting complex required for transport (ESCRT) proteins, tetraspanins, and other factors. Subsequently, during the fusion of the MVB with the cell membrane, the intraluminal vesicles (ILVs) are released outside the cell. These ILVs, typically ranging in size from 50 to 200 nm, constitute what we commonly refer to as exosomes.[14,44] Considering that both HEK-293T and Caco-2 cells are of human origin, it is reasonable to assume that the mechanisms of exosome release for these two cell types would share significant similarities. In this paper, our primary focus lies in elucidating the transport routes and kinetics of exosomes released by cells in the gut channel, towards the brain channel, and subsequent interaction of the transported exosomes with brain neuronal cells. Considering the experimental objectives, transfection efficiency, and interaction with SH-SY5Y cells, we concluded that HEK-293T cells could serve as a suitable substitute for Caco-2 cells.

We validated the expression of green fluorescence in HEK-293T cells by culturing them in a 6-well plate and transfecting them with a CD63-plasmid (Fig. 3A). To evaluate the size distribution of exosomes, we isolated exosomes from HEK-293T cells cultured in a 6-well plate in the medium and analyzed them using dynamic light scattering (DLS). The peak size was 273 nm (Fig. 3B), slightly larger than the well-established exosome size range of 50 to 200 nm.[12,13] This deviation is likely due to some exosomes aggregating during the purification process, resulting in a slightly larger size measurement. We also

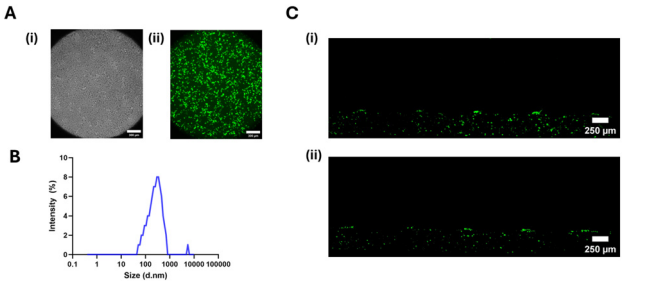

Fig. 3 HEK-293T cell CD63-GFP transfection and DLS. (A) Bright field and fluorescence images of transfected HEK-293T cell in 6well plate. (i) Bright field image of transfected HEK-293T cell in 6 well plate. (ii) Fluorescence images of transfected HEK-293T cell in 6 well plate. Scale bar 300 μm. (B) Size distribution of HEK-293T cell derived exosomes. (C) Fluorescence images of transfected HEK-293T cell in GBA-convection chip and GBA-diffusion chip. (i) Fluorescence images of transfected HEK-293T cell in GBA-convection chip. (ii) Fluorescence images of transfected HEK-293T cell in GBA-diffusion chip. Green: CD63-GFP.

confirmed consistent fluorescent expression when transfected HEK-293T cells were transferred and cultured in both the GBA-convection chip and the GBA-diffusion chip (Fig. 3C).

3.4 Transport of exosome in GBA-convection chip

We conducted experiments to confirm the transport of CD63-GFP exosomes, which were secreted by transfected HEK-293T cells in the gut channel and transported to the brain channel *via* convective flow. For comparison, we also performed the same experiment using the GBA-diffusion chip. To induce convective flow, we utilized the previously explained droplet method. Using a fluorescence microscopy, fluorescence images of exosomes in the chip were taken at 10 second intervals for 30 minutes. We analyzed the images obtained from the collagen gel channels of both the GBA-diffusion chip and GBA-convection chip over this 30 minute period, using ImageJ to track the movement path of CD63-GFP exosomes (Fig. 4A and B-i). Additionally, to compare our experimental results with a theoretical model, we employed the COMSOL Particle Trajectories module to create a particle movement model within the GBA-convection chip COMSOL model. This model allowed us to predict the movement of exosomes within the collagen gel channel.

When comparing the movement paths of CD63-GFP exosomes captured over a 30 minute period in the GBA-convection chip and the GBA-diffusion chip, a distinct difference was evident. Exosomes in the GBA-convection chip exhibited noticeable directional movement (Fig. 4A and B-i). Conversely, during the same observation period in the GBA-diffusion chip, no substantial movement of CD63-GFP exosomes towards the brain channel was observed. We tracked CD63-GFP exosomes along their recorded movement paths in the GBA-convection chip to determine the velocity of these exosomes within the collagen gel channel (Fig. 4B-ii). It was observed that a CD63-GFP exosome traversed a collagen

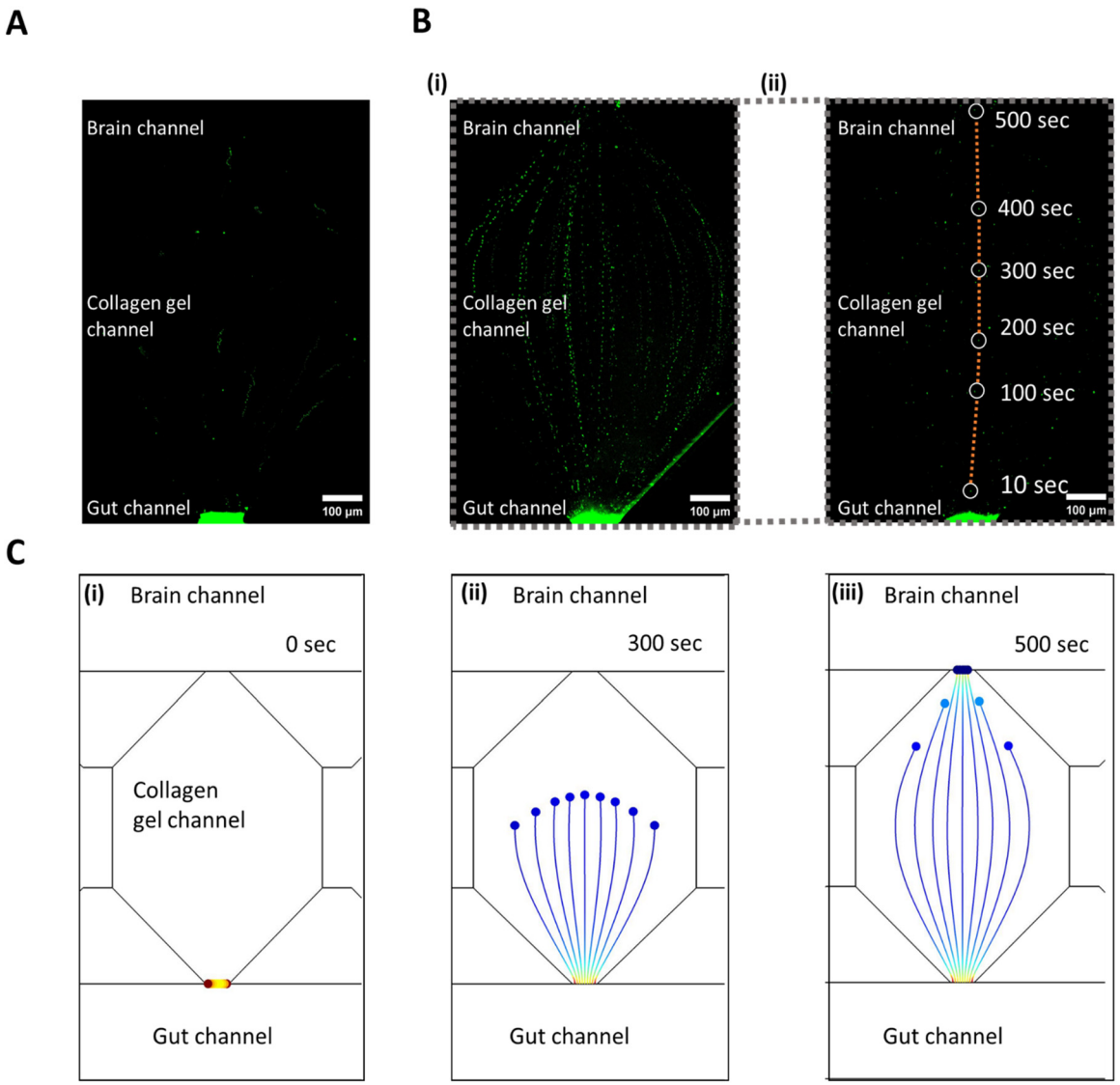

Fig. 4 CD63-GFP-exosome tracking and dynamics analysis. (A) CD63-GFP-exosomes pathways in GBA-diffusion chip collagen gel channel for 1000 seconds. (B) CD63-GFP-exosomes pathways in GBA-convection chip collagen gel channel for 1000 seconds and dynamics by time. (i) CD63-GFP exosome pathways in GBA-convection chip. (ii) CD63-GFP exosome dynamics by time. (C) GBA-convection chip COMSOL model simulation particle trajectories results.

gel channel with a length of 1300 μm in approximately 500 seconds, eventually reaching the brain channel. The average velocity of the recorded CD63-GFP exosomes was approximately 2.6 μm s^{-1}. As mentioned above, we predicted that in the human body, exosomes secreted by intestinal cells would take approximately 6–8 minutes to reach neurons in the brain. In the GBA-convection chip experiment, the implementation closely aligned with this expectation, exhibiting a similar time range. We observed that CD63-GFP exosomes exhibited directional movement within the collagen gel channel, which is likely driven by the established convective flow. To confirm this hypothesis, we conducted an analysis of CD63-GFP exosome movement using the Peclet number, a parameter that reflects the relationship between diffusion and convection.

$$\mathrm{Pe} = \frac{\text{Convective transport}}{\text{Diffusive transport}} = \frac{Lv}{D} \quad (9)$$

where L [m] and v [m s^{-1}] represent length and velocity, respectively, while D [m^2 s^{-1}] is the diffusion coefficient.[45] Calculating the Peclet number for CD63-GFP exosomes in the collagen gel channel of the GBA-convection chip yielded a value of approximately Pe = 1800. This result is consistent with the Pe = 1300 value obtained in the study by the Oh *et al.*, which examined exosome movement in collagen driven by convective flow, as mentioned previously.[24] In the GBA-convection chip, convection clearly dominates over diffusion, leading to the directional movement of CD63-GFP exosomes towards the brain channel propelled by convection.

Interstitial flow is instrumental in the transport of various substances, including proteins, drugs, and extracellular vesicles (EVs), from the bloodstream to cells in the body. Moreover, it plays a vital role in the removal of misfolded proteins and metabolic waste in the brain, which can contribute to the onset of neurological disorders.[46,47] Convection flow also aids substances in traversing the blood–brain barrier (BBB). Notably, recent research has explored convection-enhanced delivery (CED) as a therapeutic approach for brain tumors, with the aim of improving drug passage through the BBB.[47] Through *in vitro* studies on the movement of EVs and exosomes, it has become evident that convective flow is a significant driver, while diffusion-based movement plays a negligible role.[24,47] To harness the potential of EVs and exosomes as drug delivery vehicles, a comprehensive understanding of convection flow and the corresponding design considerations are essential.

We simulated the movement of CD63-GFP exosomes towards the brain channel in the GBA-convection chip using particle modelling. We incorporated a particle tracking model into the GBA-convection chip COMSOL model, and the simulations showed that particles released in the gut channel of the GBA-convection chip reached the brain channel in approximately 500 to 700 seconds (Fig. 4C). The average velocity of nine particles within the collagen gel channel of the GBA-convection chip COMSOL model was calculated at 2.4 μm s^{-1}, closely matching the results observed in the GBA-convection chip experiment for CD63-GFP exosomes. These findings suggest that our COMSOL models effectively replicates the exosome distribution pattern within the GBA chip, and it is reasonable to conclude that this model partially reflects exosome movement patterns within real human or animal systems.

Evaporation flux density can be obtained from Fick's first law of diffusion, it can derive the time-dependent radius of an evaporating droplet.[48]

$$R(t) = R_0\sqrt{1-\frac{t}{t_{ev}}} \tag{10}$$

$$t_{ev} = \frac{{R_0}^2}{2D\left(\frac{C_{sat}}{C_w}\right)(1-\mathrm{RH})} \tag{11}$$

where R_0 [m] is the initial droplet radius, t_{ev} [s] is the droplet evaporation time, D [m^2 s^{-1}] is the diffusion coefficient of water vapor in air, C_w [mol L^{-1}] is the number density of liquid water, C_{sat} [mol L^{-1}] is the saturation concentration of water, and RH is the relative humidity.

$$C_{sat} = \frac{P_{sat}M}{RT[\mathrm{K}]} \tag{12}$$

$$\log_{10}P_{sat} = A - \frac{B}{C + T[^\circ\mathrm{C}]} \tag{13}$$

where P_{sat} [mmHg] is the saturated water vapor pressure, M [kg mol^{-1}] is the molar mass of water, R [J mol^{-1} K^{-1}] is the gas constant, T [K] is the absolute temperature, and A, B, and C are the parameters of the Antoine equation. T [°C] is the temperature in degrees Celsius.[49]

As described by eqn (11), the evaporation time t_{ev} is dependent on RH, indicating that adjusting RH can either suppress or enhance droplet evaporation for instance, the evaporation time of a droplet with an initial radius R_0 = 3.01 mm, at a temperature of 36 °C and a RH of 90%, can be calculated using eqn (11) through (13). In eqn (13), with T = 36 °C and using the Antonie equation parameters A = 8.08, B = 1705, and C = 240, the saturation pressure P_{sat} is calculated to be 44.7 mmHg.[49] Substituting this value into eqn (12) yields a saturation concentration C_{sat} of approximately 0.0417 mol L^{-1}. In eqn (11), using the values for D = 2.36 × 10–5 m^2 s^{-1} and C_w = 55.40 mol L^{-1} from prior studies,[48,50] and substituting a RH of 0.9 and an initial radius R_0 = 3.01 mm, the evaporation time t_{ev} is calculated to be approximately 670 hours. At 90% RH, evaporation is nearly negligible over a 24 hour period, influencing the droplet radius and leading to a consistent change in fluid velocity.

S. Seo *et al.* maintained a RH of 95% by placing a microfluidic chip inside the Chamlide TC incubator (Live Cell Instrument) and observed evaporation-driven transport control of small molecules within the microfluidic chip through the regulation of evaporation.[51] Alternatively, E. Berthier *et al.* demonstrated that placing 12 water-filled Petri dishes in a Bioassay Tray (NUNC, Rochester, NY) within a 36 °C cell culture incubator resulted in an RH exceeding 90%.[52] Given that maintaining RH at 90% is feasible under standard laboratory conditions, it is expected that suppression of evaporation within the GBA-chip will ensure stable fluid flow rates, enabling the observation of exosome movement and interactions.

3.5 Exosome interaction with neuroblastoma cells

Using the GBA-convection chip, we observed the transport of CD63-GFP exosomes from HEK-293T cells in the gut channel towards the brain channel and subsequent attachment at the

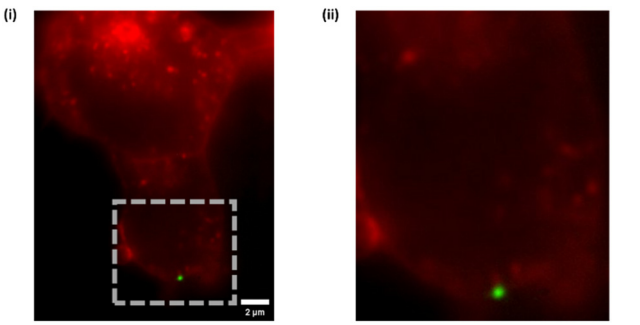

Fig. 5 Transfected HEK-293T cell CD63-GFP-exosome interaction with SH-SY5Y. (i) CD63-GFP-exosomes through collagen gel channel and SH-SY5Y membrane merged image. (ii) Enlarged view of the gray dashed box region in (i). Red: SH-SY5Y cell membrane. Green: Transfected HEK-239T cell CD63-GFP-exosome.

membrane of SH-SY5Y cells (Fig. 5). While monitoring CD63-GFP exosomes reaching the membrane of SH-SY5Y cells and observing them for 1 minute, we noticed a gradual loss of GFP-exosome intensity, and eventually disappearing form the initial location. Recipient cells can uptake exosomes secreted by donor cells through three primary mechanisms.[44] The first mechanism involves exosomes from donor cells binding to receptors present on the recipient cell membrane, thereby transmitting signals. The second mechanism entails exosomes from donor cells fusing with the recipient cell membrane, facilitating the transfer of proteins, nucleic acids, and other contents. The third mechanism encompasses the uptake of exosomes from donor cells by recipient cells, followed by the degradation of donor cell exosomes by the recipient cell's lysosomes. This process releases internal proteins, nucleic acids, and other contents, which are then delivered to the recipient cells.[44] Teresa Vilanova-Perez *et al.* conducted experiments involving the introduction of exosomes from HEK-293T cells to mammalian sperm, observing the effects over time. Their results indicated that the internalization of exosomes from HEK-293T cells by mammalian sperm occurred 10 minutes later.[53] In another study, Oh *et al.* observed that undifferentiated F11 cells take up exosomes from differentiated F11 cells within 3 minutes.[24] Moreover, previous studies have provided evidence that SH-SY5Y cells are proficient in internalizing CD63-GFP exosomes derived from transfected HEK-293T cells.[43] In the GBA-convection chip, we believe that CD63-GFP exosomes from transfected HEK-293T cells interacted with the membranes of SH-SY5Y cells, either by attaching and transmitting signals or by fusing with the membranes. In accordance with preceding research, exosomes demonstrate distinctive dynamics during their attachment to the plasma membrane of recipient cells and as they traverse towards the cellular interior, ultimately binding with lysosomes. The reported velocities, drift velocities, and diffusion coefficients during plasma membrane attachment are approximately 0.1 $\mu m\ s^{-1}$, 0.01 $\mu m\ s^{-1}$, and 0.002 $\mu m^2\ s^{-1}$, respectively. Conversely, velocities, drift velocities, and diffusion coefficients for exosome movement towards the cellular interior, culminating in lysosomal binding, are reported as 0.2 $\mu m\ s^{-1}$, 0.05 $\mu m\ s^{-1}$, and 0.05 $\mu m^2\ s^{-1}$, respectively.[54] In future studies, we expect that investigating exosome dynamics near the plasma membrane, building upon previous research, and utilizing optical tweezers to measure the force between a single exosome and the SH-SY5Y cell membrane will aid in predicting their binding structure and enhancing our understanding of their interaction.

4. Conclusions

To establish an *in vitro* model emulating the GBA, we co-cultured intestinal cells and brain neural cells on opposing sides of the collagen gel channel in the GBA-convection chip. The use of FITC-dextran confirmed the generation of convection within the GBA-convection chip, facilitating the transport of substances from the gut channel to the brain channel. Taking advantage of this convection flow, we monitored the migration of CD63-GFP exosomes, secreted from the gut channel, as they transited the collagen gel channel and reached the SH-SY5Y cells. Additionally, we developed and evaluated a COMSOL simulation model. SW480 cells are human colorectal cancer cell lines, like Caco-2 cells. Previous studies have utilized transfection to label the exosome surface marker CD81 with RFP, facilitating the imaging of exosome release processes in intestinal cells.[55] Consequently, SW480 cells are anticipated to be valuable for research involving our GBA-convection chip and GBA-exosome studies. Based on these results, we believe that the GBA-convection chip holds promise for advancing the application of exosomes as signalling mediators in GBA interactions and as potential agents for drug delivery in the context of neurological disorders.

Data availability

Data are available upon request from the authors.

Author contributions

Conceptualization, G. M. S., J. H. S., and D. K.; methodology, G. M. S. and Y. J. K.; experiment, G. M. S. and H. L. software analysis, G. M. S.; validation, J. H. S. and D. K.; data analysis, G. M. S. and H. L.; resources, D. K. and J. H. S.; writing, all authors contributed with first draft prepared by G. M. S.

Conflicts of interest

There are no conflicts to declare.

Acknowledgements

This work was supported by the Basic Research Lab (2022R1A4A2000748) and the Bio & Medical Technology Development Program (2022M3A9B6018217) by the National Research Foundation of Korea, the Alchemist Project of the Korea Evaluation Institute of Industrial Technology (KEIT 20018560, NTIS 1415184668) by the Ministry of Trade, Industry & Energy (MOTIE), Republic of Korea, the Korea Institute of Marine Science & Technology Promotion (KIMST) funded by the Ministry of Oceans and Fisheries, Korea (RS-2024-00402200), and the Hongik University Research Fund.

References

1 N. Hattori and Y. Yamashiro, *Ann. Nutr. Metab.*, 2021, 1–3.
2 B. Dalile, L. V. Oudenhove, B. Vervliet and K. Verbeke, *Nat. Rev. Gastroenterol. Hepatol.*, 2019, **16**, 461–478.
3 N. A. Pizarroso, P. Fuciños, C. Gonçalves, L. Pastrana and I. R. Amado, *Nutrients*, 2021, **13**, 632.
4 J. F. Cryan, K. J. O'Riordan, C. S. M. Cowan, K. V. Sandhu, T. F. S. Bastiaanssen, M. Boehme, M. G. Codagnone, S. Cussotto, C. Fulling, A. V. Golubeva, K. E. Guzzetta, M.

Jaggar, C. M. Long-Smith, J. M. Lyte, J. A. Martin, A. Molinero-Perez, G. Moloney, E. Morelli, E. Morillas, R. O'Connor, J. S. Cruz-Pereira, V. L. Peterson, K. Rea, N. L. Ritz, E. Sherwin, S. Spichak, E. M. Teichman, M. van de Wouw, A. P. Ventura-Silva, S. E. Wallace-Fitzsimons, N. Hyland, G. Clarke and T. G. Dinan, *Physiol. Rev.*, 2019, **99**, 1877–2013.

5 D. Cammann, Y. Lu, M. J. Cummings, M. L. Zhang, J. M. Cue, J. Do, J. Ebersole, X. Chen, E. C. Oh, J. L. Cummings and J. Chen, *Sci. Rep.*, 2023, **13**, 5258.

6 S. Trapp and D. I. Brierley, *Br. J. Pharmacol.*, 2022, **179**, 557–570.

7 G. Monti, D. G. Moreira, M. Richner, H. A. M. Mutsaers, N. Ferreira and A. Jan, *Cells*, 2022, **11**, 2023.

8 H. Li, J. Sun, F. Wang, G. Ding, W. Chen, R. Fang, Y. Yao, M. Pang, Z.-Q. Lu and J. Liu, *Brain Res.*, 2016, **1642**, 70–78.

9 C. Willyard, *Nature*, 2021, **590**, 22–25.

10 T. Bartels, J. G. Choi and D. J. Selkoe, *Nature*, 2011, **477**, 107–110.

11 S. G. Chen, V. Stribinskis, M. J. Rane, D. R. Demuth, E. Gozal, A. M. Roberts, R. Jagadapillai, R. Liu, K. Choe, B. Shivakumar, F. Son, S. Jin, R. Kerber, A. Adame, E. Masliah and R. P. Friedland, *Sci. Rep.*, 2016, **6**, 34477.

12 M. Clapp, N. Aurora, L. Herrera, M. Bhatia, E. Wilen and S. Wakefield, *Clin. Pract.*, 2017, **7**, 987.

13 G. van Niel, G. D'Angelo and G. Raposo, *Nat. Rev. Mol. Cell Biol.*, 2018, **19**, 213–228.

14 J. M. Shin, C. Lee, S. Son, C. H. Kim, J. A. Lee, H. Ko, S. Shin, S. H. Song, S. Park, J. Bae, J. Park, E. Choe, M. Baek and J. H. Park, *Adv. Sci.*, 2021, e2103245.

15 M. T. Roefs, J. P. G. Sluijter and P. Vader, *Trends Cell Biol.*, 2020, **30**, 990–1013.

16 C. C. Chen, L. Liu, F. Ma, C. W. Wong, X. E. Guo, J. V. Chacko, H. P. Farhoodi, S. X. Zhang, J. Zimak, A. Ségaliny, M. Riazifar, V. Pham, M. A. Digman, E. J. Pone and W. Zhao, *Cell. Mol. Bioeng.*, 2016, **9**, 509–529.

17 W. A. Banks, P. Sharma, K. M. Bullock, K. M. Hansen, N. Ludwig and T. L. Whiteside, *Int. J. Mol. Sci.*, 2020, **21**, 4407.

18 G. C. Terstappen, A. H. Meyer, R. D. Bell and W. Zhang, *Nat. Rev. Drug Discovery*, 2021, **20**, 362–383.

19 H. Peng, W. Ji, R. Zhao, J. Yang, Z. Lu, Y. Li and X. Zhang, *J. Mater. Chem. B*, 2020, **8**, 7591–7608.

20 M.-H. Kim, D. van Noort, J. H. Sung and S. Park, *Int. J. Mol. Sci.*, 2021, **22**, 13513.

21 R. Inotsuka, M. Udono, A. Yamatsu, M. Kim and Y. Katakura, *Nutrients*, 2021, **13**, 2544.

22 X.-D. Chen, J. Zhao, X. Yang, B.-W. Zhou, Z. Yan, W.-F. Liu, C. Li and K.-X. Liu, *Mol. Neurobiol.*, 2021, **58**, 4828–4841.

23 D. E. Ingber, *Nat. Rev. Genet.*, 2022, **23**, 467–491.

24 H. J. Oh, Y. Shin, S. Chung, D. W. Hwang and D. S. Lee, *Biomaterials*, 2017, **112**, 82–94.

25 M.-H. Kim, D. Kim and J. H. Sung, *J. Ind. Eng. Chem.*, 2021, **101**, 126–134.

26 W. J. Polacheck, J. L. Charest and R. D. Kamm, *Proc. Natl. Acad. Sci. U. S. A.*, 2011, **108**, 11115–11120.

27 U. Nam, S. Kim, J. Park and J. S. Jeon, *Micromachines-Basel*, 2020, **11**, 747.

28 I.-J. Chen, E. C. Eckstein and E. Lindner, *Lab Chip*, 2008, **9**, 107–114.

29 T. Kihara, J. Ito and J. Miyake, *PLoS One*, 2013, **8**, e82382.

30 H. J. Oh, J. Kim, H. Park, S. Chung, D. W. Hwang and D. S. Lee, *Biosens. Bioelectron.*, 2019, **126**, 647–656.

31 K. Brennan, K. Martin, S. P. FitzGerald, J. O'Sullivan, Y. Wu, A. Blanco, C. Richardson and M. M. M. Gee, *Sci. Rep.*, 2020, **10**, 1039.

32 D. Gupta, X. Liang, S. Pavlova, O. P. B. Wiklander, G. Corso, Y. Zhao, O. Saher, J. Bost, A. M. Zickler, A. Piffko, C. L. Maire, F. L. Ricklefs, O. Gustafsson, V. C. Llorente, M. O. Gustafsson, R. B. Bostancioglu, D. R. Mamand, D. W. Hagey, A. Görgens, J. Z. Nordin and S. E. Andaloussi, *J. Extracell. Vesicles*, 2020, **9**, 1800222.

33 C. Hall, E. Lueshen, A. Mošat' and A. A. Linninger, *J. Pharm. Sci.*, 2012, **101**, 1221–1241.

34 L. A. Ray and J. J. Heys, *Fluids*, 2019, **4**, 196.

35 R. Li, J. C. Serrano, H. Xing, T. A. Lee, H. Azizgolshani, M. Zaman and R. D. Kamm, *Mol. Biol. Cell*, 2018, **29**, 1927–1940.

36 C. Qin, S. Zhang, Q. Yuan, M. Liu, N. Jiang, L. Zhuang, L. Huang and P. Wang, *Chemosens*, 2022, **10**, 173.

37 C. P. Epperla, N. Mohan, C. Chang, C. Chen and H. Chang, *Small*, 2015, **11**, 6097–6105.

38 R. Kalluri and V. S. LeBleu, *Science*, 2020, **367**(6478), DOI: **10.1126/science.aau6977**.

39 B. S. Joshi, M. A. de Beer, B. N. G. Giepmans and I. S. Zuhorn, *ACS Nano*, 2020, **14**, 4444–4455.

40 C. P. Lai, O. Mardini, M. Ericsson, S. Prabhakar, C. A. Maguire, J. W. Chen, B. A. Tannous and X. O. Breakefield, *ACS Nano*, 2014, **8**, 483–494.

41 R. Kojima, D. Bojar, G. Rizzi, G. C.-E. Hamri, M. D. El-Baba, P. Saxena, S. Ausländer, K. R. Tan and M. Fussenegger, *Nat. Commun.*, 2018, **9**, 1305.

42 Y. Jahangard, H. Monfared, A. Moradi, M. Zare, J. Mirnajafi-Zadeh and S. J. Mowla, *Front. Neurosci.*, 2020, **14**, 564.

43 B. J. Jurgielewicz, Y. Yao and S. L. Stice, *Nanoscale Res. Lett.*, 2020, **15**, 170.

44 M. Mathieu, L. Martin-Jaular, G. Lavieu and C. Théry, *Nat. Cell Biol.*, 2019, **21**, 9–17.

45 C.-L. Jaime, S. Winnie, D. Maria, A. Valentina, A. Muhammad, M. Sandrine, N. Christiane and G. D. Kipling, Lab-on-a-Chip Devices and Micro-Total Analysis Systems: A Practical Guide, 2015, DOI: **10.1007/978-3-319-08687-3**.

46 C. A. Stine and J. M. Munson, *Front. Oncol.*, 2019, **9**, 966.

47 P. A. Sariano, R. R. Mizenko, V. S. Shirure, A. K. Brandt, B. B. Nguyen, C. Nesiri, B. S. Shergill, T. Brostoff, D. M. Rocke, A. D. Borowsky, R. P. Carney and S. C. George, *J. Extracell. Vesicles*, 2023, **12**, e12323.

48 A. Božič and M. Kanduč, *J. Biol. Phys.*, 2021, **47**, 1–29.

49 Y. Hasegawa, W. Matsuura, C. Abe and A. Ikeda, *Membranes*, 2021, **11**, 347.

50 G. Badino, *J. Cave Karst Stud.*, 2009, **71**, 100–107.

51 S. Seo, D. Ha and T. Kim, *Nat. Commun.*, 2021, **12**, 1336.

52 E. Berthier, J. Warrick, H. Yu and D. J. Beebe, *Lab Chip*, 2008, **8**, 852–859.
53 T. Vilanova-Perez, C. Jones, S. Balint, R. Dragovic, M. L. Dustin, M. Yeste and K. Coward, *Nanomedicine*, 2020, **15**, 1965–1980.
54 T. Tian, Y. Zhu, F. Hu, Y. Wang, N. Huang and Z. Xiao, *J. Cell. Physiol.*, 2013, **228**, 1487–1495.
55 O. Oleksiuk, M. Abba, K. C. Tezcan, W. Schaufler, F. Bestvater, N. Patil, U. Birk, M. Hafner, P. Altevogt and C. Cremer, *Onco Targets Ther*, 2015, **6**, 44745.